Point-by-point inscription of first-order fiber Bragg grating for C-band applications

Y. Lai, K. Zhou, K. Sugden, I. Bennion

Photonics Research Group, School of Engineering and Applied Science, Aston University, Birmingham, B4 7ET, UK
Lai_yicheng@dsi.a-star.edu.sg

Abstract: The influence of the fiber geometry on the point-by-point inscription of fiber Bragg gratings using a femtosecond laser is highlighted. Fiber Bragg gratings with high spectral quality and strong first-order Bragg resonances within the C-band are achieved by optimizing the inscription process. Large birefringence (1.2×10^{-4}) and high degree of polarization-dependent index modulation are observed in these gratings. Potential applications of these gratings in resonators are further illustrated.

OCIS codes: (060.3735) Fiber Bragg gratings; (080.2468) First-order optics; (260.1440) Birefringence; (230.5750) Resonators

References

1. B. Malo, K.O. Hill, F. Bilodeau, D.C. Johnson, J. Albert, "Point-by-point fabrication of micro-Bragg gratings in photosensitive fiber using single excimer pulse refractive index modification techniques," Electron. Lett. **29**, 1668-1669 (1993).
2. Y. Lai, A. Martinez, I. Khrushchev, I. Bennion, "Distributed Bragg reflector fiber laser fabricated by femtosecond laser inscription," Opt. Lett. **31**, 1672-1674 (2006).
3. N. Jovanovic, A. Fuerbach, G.D. Marshall, M.J. Withford, S.D. Jackson, "Stable high-power continuous-wave Yb3+-doped silica fiber laser utilizing a point-by-point inscribed fiber Bragg grating," Opt. Lett. **32**, 1486-1489 (2007).
4. Y. Cheng, K. Sugioka, K. Midorikawa et al, "Control of the cross-sectional shape of a hollow microchannel embedded in photostructurable glass by use of a femtosecond laser," Opt. Lett. **28**, 55-57 (2003).
5. F. Hindle, E. Fertein, C. Przygodzki et al, "Inscription of long period gratings in pure silica and germo-silicate fiber cores by femtosecond laser irradiation," IEEE Photon. Technol. Lett. **16**, 1861-1863 (2004).
6. A. Martinez, M. Dubov, I. Khrushchev, I. Bennion, "Direct writing of fiber Bragg gratings by femtosecond laser," Electron. Lett. **40**, 1170-1172 (2004).
7. Y. Lai, K. Zhou, L. Zhang, I. Bennion, "Micro-channels in conventional single-mode fibers," Opt. Lett. **31**, 2559-2561 (2006).
8. K.M. Davies, K. Miura, N. Sugimoto, K. Hirao, "Writing waveguides in glass with a femtosecond laser," Opt. Lett. **21**, 1729-1731 (1996).
9. P. Lu, D. Grobnic, S.J. Mihailov, "Characterization of the birefringence in fiber Bragg gratings fabricated with an ultra-fast infrared laser," J. Lightwave Tech. **25**, 779-786 (2007).
10. H. Zhang, S.M. Eaton, J. Li, P.R. Herman, "Femtosecond laser direct writing of multiwavelength Bragg grating waveguides in glass," Opt. Lett. **31**, 3495-3497 (2006).
11. M. Ibsen, E. Ronnekleiv, G.J. Cowle, M.O. Berendt, O. Hadeler, M.N. Zervas, R.I. Laming, "Robust high power (>20mW) all-fiber DFB lasers with unidirectional and truly single polarization outputs," in *Conference on Lasers and Electro-Optics*, paper CWE4, 245-246 (1999).

1. Introduction

The use of intense femtosecond laser pulses to create permanent refractive index change in glass materials has led to recent interest in fiber Bragg grating (FBG) fabrications based on this technique. By means of focusing the femtosecond laser pulses into the fiber core, point-by-point (PBP) Bragg grating inscription can be further achieved without the need of a phase mask. The grating period, defined by the periodicity of the laser-modified volumes, is simply the ratio of the translation speed of the fiber to the laser pulse repetition rate. Bragg

#89342 - $15.00 USD Received 2 Nov 2007; revised 14 Dec 2007; accepted 15 Dec 2007; published 20 Dec 2007

wavelengths can hence be fully controlled to provide resonances within the desired range. Such direct inscription technique has been demonstrated previously to achieve C-band fiber Bragg reflectors operating in second or third-order, and has been further adopted to create grating resonators at various useful wavelengths [1-3].

To date, the point-by-point FBG fabrications have rely on higher order grating structures to achieve strong, quality spectral resonances at the desired Bragg wavelength. On the other hand, for a fixed inscribed length and index modulation, one can expect the Bragg response from its first-order grating structure to be more pronounced than that from a grating operating in the higher order since the number of constituent periods is reduced for the latter. The inscription length and pulse energy required to achieve a particular grating reflectivity can therefore be reduced significantly in a first-order grating formation. It is also known that the mechanism of index modification through femtosecond laser inscription involves a nonlinear process and the size of the region which the refractive index changes occur can be much smaller than the spot size of the focused beam. The photo-induced index change occurs largely in the focal region where the light intensity is above a defined threshold, thus allowing the modified feature size to be below the diffraction limit [4, 5]. As a result, with appropriate control on the pulse energy and the focusing geometry in a PBP grating inscription, one can anticipate the achievable effective index modification size to be sufficiently small for grating periods with first-order Bragg resonance in the C-band. However, such FBGs fabricated to date only reveal resonances of modest strength with undesired spectral distortions [6]. Furthermore, on the contrary, the Bragg response from the higher order grating structure outperforms that from its first-order counterpart.

In this paper, we demonstrate PBP inscription of FBGs in conventional single-mode fiber (Corning SMF-28) with first-order Bragg resonances within the C-band using an IR femtosecond laser. The inscription conditions to optimize the grating fabrication have been explored to achieve first-order Bragg resonances of good spectral quality. We first highlight the distortion effect that the intrinsic fiber geometry has on an incident focused femtosecond laser beam during PBP grating inscription. The fabrication limitation was then alleviated to allow inscription of strong, short-length FBGs using low (75nJ) pulse energy. In comparison to FBGs based on PBP inscription technique, the measured birefringence and polarization-dependent reflectivity in these FBGs are of a magnitude not observed before. Further comparisons to second-order grating structures were carried out and potential applications of these fiber gratings in resonator cavities are further illustrated.

2. Experiment

An amplified Ti:Sapphire laser system producing 150fs pulses at 800nm at a repetition rate of 1kHz was focused into the fiber by a 100× microscopic objective that has a NA of 0.55 and a working distance of 13mm. The fiber was placed on a stable, high precision (2nm resolution), air bearing translation stage moving at a constant speed along the fiber axis so that each laser pulse produces a grating pitch in the fiber core at the focal point of the beam. No photosensitization to the fiber was carried out prior to the exposure.

It has been shown that the intrinsic fiber surface curvature can cause significant distortion to an incident focused femtosecond beam [7]. To help visualize the distortion effect in a grating inscription process, a number of 3mm-long grating structures were fabricated into both the fiber cladding and the fiber core. The first grating was inscribed near to the cladding-air interface while subsequent gratings were then progressively placed closer towards the fiber core. The fiber was translated at 3mm/sec to create 3μm grating period and the measured pulse energy used was 400nJ. The gratings fabricated were then viewed under a 40× microscope lens and four of the gratings are shown in Fig. 1.

It is clear that the grating fringes vary and distort as the laser focus is positioned closer towards the fiber core. More importantly, the fringe visibility decreases drastically to a point that the grating structure within the fiber core is no longer visible. As in [7], the surface curvature of fiber introduces a cylindrical lens effect to the incident beam leading to differential focusing conditions to the orthogonal planes of the incident femtosecond pulse.

#89342 - $15.00 USD Received 2 Nov 2007; revised 14 Dec 2007; accepted 15 Dec 2007; published 20 Dec 2007

Such distortion increases as the focal point moves closer towards the fiber core. The decrease in visibility of the laser-induced features indicates that the laser energy is distributed over a larger focal volume, hence lowering the intensity for inducing significant index modification. Periodic index modulation formation is further hindered by the overlapping of the laser focal volumes. Consequently, the distortion to the incident pulses severely limits the grating order achievable, particularly for closely-spaced grating periods.

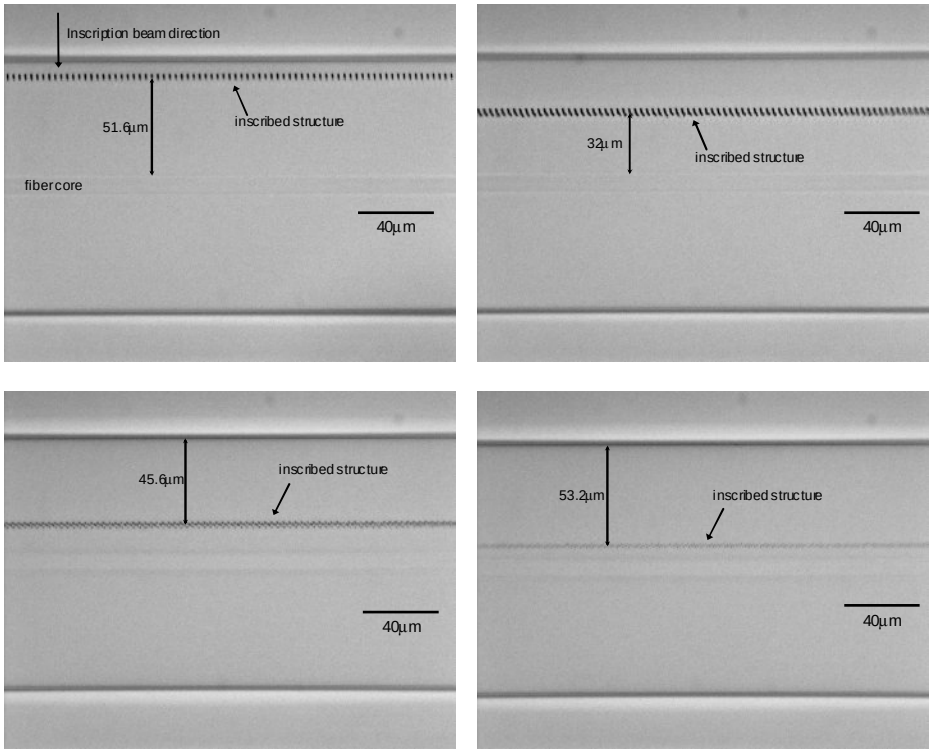

Fig. 1. Microscope images of 3μm-period grating structures in a single-mode fiber where the inscription laser focus is positioned at different distances from the core. The fringe visibility and intensity of the gratings decrease as the laser focus is positioned closer towards the core.

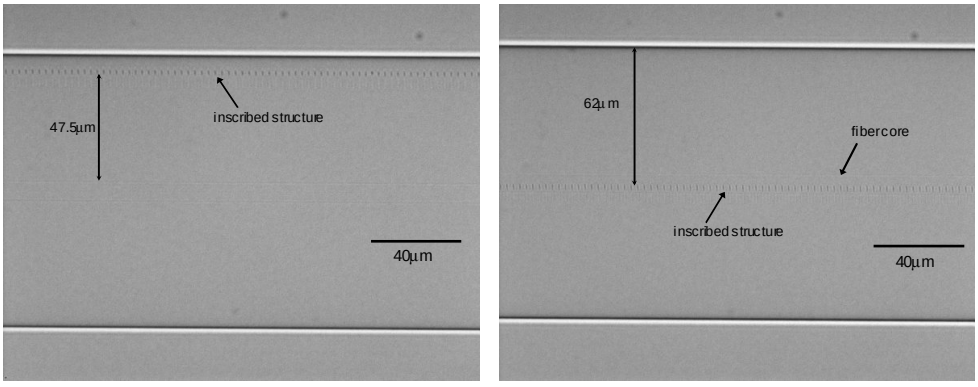

Fig. 2. Microscope images of 3μm-period grating structures inscribed in a single-mode fiber using 120nJ pulse energy. Distortion to the inscription laser beam due to the fiber surface geometry was alleviated during fabrication. The grating structures remain consistent regardless the positions of the beam focus within the fiber.

#89342 - $15.00 USD Received 2 Nov 2007; revised 14 Dec 2007; accepted 15 Dec 2007; published 20 Dec 2007

To overcome the fabrication limitation imposed by the intrinsic fiber geometry, the fiber was placed within a square micro-capillary tube filled with index-matching oil so that the surface geometry presented to the path of the incident femtosecond laser beam is flat [7]. Conceptually similar to the use of an oil-immersion lens, the approach however does not restrict fabrication flexibility and is easily implemented within the current fabrication system. The fabrication process was similarly repeated except the pulse energy required to enable good fringe visibility under the microscope for all gratings can be reduced to 120nJ. The resultant grating structures fabricated are as shown in Fig. 2.

It is evident that there are no observable distortions to the inscribed structures as a function of the position of the beam focus within the fiber. The fringe visibility remains consistent and clearly defined for all gratings. The square capillary tube has effectively alleviated the limitations imposed by the surface geometry of fiber to preserve the tight focusing conditions of the incident pulse. Without spatial dispersal of the focal volume, periodic index modulation remains readily visible for grating structures inscribed into the core region using such low pulse energy.

To exemplify the tight focusing conditions and highly-localized index modification region achievable, in a separate experiment, a 5mm-long grating was inscribed into the fiber core using a translation speed of 0.539mm/sec with measured pulse energy of 75nJ. This led to a grating period of 0.539μm with a first-order Bragg resonance at ~1561nm. The inscription process took approximately 10 seconds to complete and the inscribed grating structure viewed under the 100× microscope lens is shown in Fig. 3(a). The laser-formed grating consists of an array of individual ellipsoidal index perturbation, each formed by a single laser pulse, with observed width and depth of <0.3μm and ~1.9μm respectively (aspect ratio of 6.3). In line with previous studies [4, 8], these inscribed elliptical features are attributed to the longitudinal distribution of the spatial intensity of the beam focused by an objective lens. The aspect ratio of the observed inscribed feature depends on the ratio of the Rayleigh length to the beam waist at focus and reflects the energy distribution in the vicinity of the laser focus. Despite the close proximity of the grating fringes, the ~0.54μm periodic index modulation is readily visible.

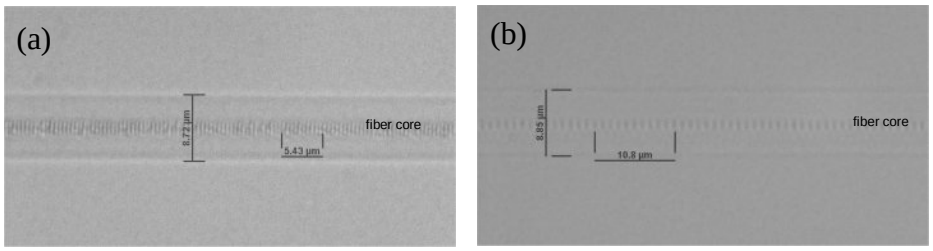

Fig. 3. Microscope images of (a) a first-order Bragg grating structure and, (b) a second-order Bragg grating structure, inscribed in standard single-mode fibers. Note that the measurement resolution is limited to 0.1μm.

The asymmetry of the induced index profile with respect to the circular cross-sectional area of the fiber core suggests that the grating would exhibit polarization-dependent spectral responses. Using a polarized light source and a high-resolution optical spectrum analyzer, the transmission profiles of the grating along orthogonal polarization states are measured and the normalized results are fitted to simulations based on the transfer matrix method as shown in Fig. 4. Even though the 1st order grating model under the transfer matrix method is not an exact representation of the inscribed grating structure, the comparison of the measured transmission profile to the simulated counterpart allows the induced refractive index change to be inferred. The difference in Bragg wavelengths, $\Delta\lambda_{pol}$, between the orthogonal polarization spectral profiles measured 0.13nm, corresponding to an effective birefringence, Δn_{eff}, on the

#89342 - $15.00 USD Received 2 Nov 2007; revised 14 Dec 2007; accepted 15 Dec 2007; published 20 Dec 2007

order of 1.2×10^{-4}. The effective index modulation, δn, along each polarization state, are 4.06×10^{-4} and 3.17×10^{-4} corresponding to grating strength parameter, κL, of ~4.09 and ~3.19 respectively. This leads to a difference in transmission dips at Bragg wavelengths of 7.8dB ($\Delta\delta n$ ~0.89×10^{-4}). Such pronounced polarization characteristics are more than an order of magnitude larger than conventional UV-inscribed uniform FBGs in standard SMF and we believe such degrees of polarization-dependency have not been observed in previous studies of PBP femtosecond laser inscribed uniform FBGs. It is worthwhile to note that such degrees of polarization dependency are similarly observed in FBGs fabricated using femtosecond laser exposure through a phase mask [9]. We believe that the ellipsoidal index profile that constitutes the grating pitches, analogous to grating inscribed in an elliptical core birefringent fiber, accounts largely for the polarization-characteristics of the FBGs. Based on the microscope images, the tilt of the grating fringes with respect to the fiber axis is not appreciable to take account of the polarization sensitivity.

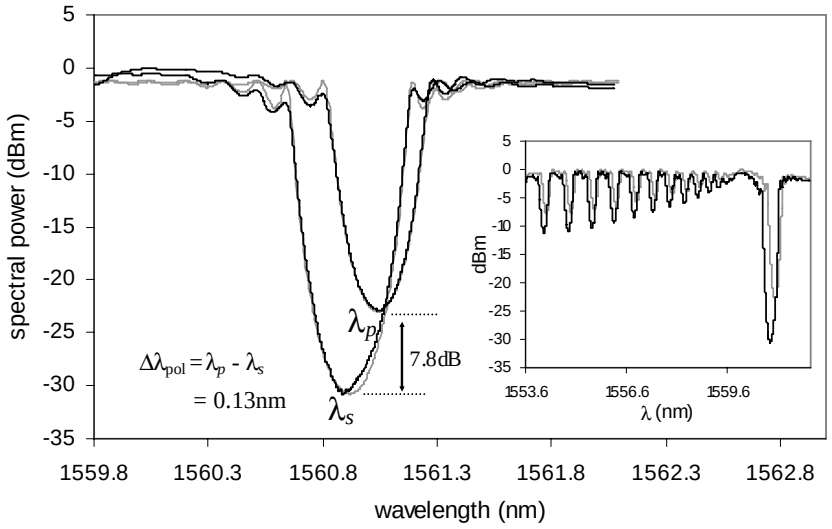

Fig. 4. Superimposed measured and simulated (grey) spectral transmission profiles of the first-order fiber Bragg grating along orthogonal polarization states. The Bragg wavelengths at orthogonal polarization states are denoted as λ_s and λ_p respectively. Inset shows the measured spectra profiles which highlight the short wavelength lossy cladding modes. Note that the spectral profile along the *p*-polarization is drawn in grey.

Compared to previous reports, the low inscription energy required and high index modulation achieved here for the first-order C-band Bragg resonance highlighted the improved index modification confinement attained under such focusing conditions. The absence of any subsidiary resonance peaks around the Bragg resonance exemplifies the uniformity of the grating period over its 5mm length. The distortion effect due to the curvature of the fiber surface is evidently a key limiting factor in the direct inscription of low-order fiber grating structures. It is worth noting that the out-of-band loss of the grating fabricated is less than 1dB. The higher loss of the grating, as compared to conventional UV-inscribed gratings, can be attributed to the optical scattering by the small inscribed volume relative to the large mode diameter. By changing the fiber scan speed, Bragg resonances can be provided anywhere in the C-band and such distinct birefringence and polarization-dependent reflectivity characteristics are consistently observed.

As mentioned, for a fixed inscribed length and grating index modulation (i.e. identical pulse energy), one can expect the Bragg resonance from its first-order grating structure to be more pronounced than that from a grating operating in the higher order. To illustrate this point, a 5mm-long second-order grating structure (translation speed =1.078mm/sec) was

#89342 - $15.00 USD Received 2 Nov 2007; revised 14 Dec 2007; accepted 15 Dec 2007; published 20 Dec 2007

inscribed under the same fabrication conditions (pulse energy at 75nJ). The microscope image of the grating and its spectral profiles along orthogonal polarization states are as shown in Fig. 3(b) and Fig. 5(a) respectively. The grating's second-order Bragg resonance at ~1560.9nm is evidently weaker and the effective birefringence and differential index modulation along orthogonal polarization states are less pronounced at $\Delta n_{eff} \sim 2.9\times10^{-5}$ ($\Delta\lambda_{pol}$ ~0.032nm) and $\Delta\delta n \sim 0.12\times10^{-4}$ respectively. The inscription was then repeated using increased pulse energy of 105nJ to increase the grating's reflectivity and the measured transmission spectral responses are as shown in Fig. 5(b). The corresponding increase in its Bragg wavelength and polarization characteristics, namely $\Delta n_{eff} \sim 6.9\times10^{-5}$ ($\Delta\lambda_{pol}$ ~0.074nm) and $\Delta\delta n \sim 0.23\times10^{-4}$, are observed but they remain considerably less than that in a first-order grating configuration. Such observations are consistently obtained over several separate fabrications.

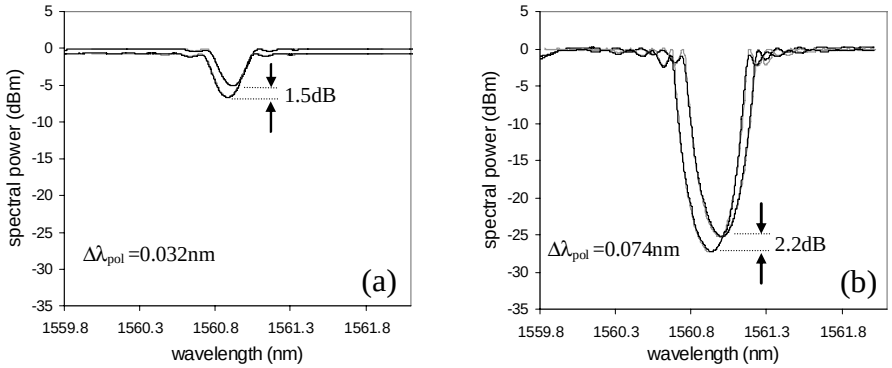

Fig. 5. Superimposed measured and simulated (grey) transmission spectral profiles along orthogonal polarization states of second-order fiber Bragg gratings fabricated using (a) 75nJ and, (b) 105nJ. The difference between Bragg wavelengths along orthogonal polarizations is denoted as $\Delta\lambda_{pol}$. All spectra profiles are scaled identically for comparison.

Comparing the 1st order and 2nd order FBG structures fabricated under identical laser intensity, it is intuitive to expect the proximity of the grating pitches to have a profound effect on the dc refractive index, hence Bragg wavelength, as well as the polarization characteristics. For the 1st order grating structure, the spacing between adjacent laser-induced perturbations (grating period) is much closer compared to its 2nd order counterpart. The close proximity leads to a partial overlapping of the grating pitches, raising the effective refractive index over one grating period. The presence of the 1st order Bragg resonance however indicates the existence of high index modulation in the grating structure. This highlights the fact that each laser-induced grating pitch consists of a central region of high index modification with a small surrounding region of lower index modification. Note that without further detail measurements, the exact sign of the index modifications are unknown at present. When these laser-induced perturbations are spaced further apart in a 2nd order FBG formation, the overlap between adjacent grating pitches is greatly reduced and the effective refractive index over one grating period decreases to lead to a lower Bragg resonance wavelength. Consequently, the 1st order Bragg wavelength from the 1st order grating structure was measured to be higher than the Bragg wavelength of the grating operating in 2nd order. Such observations on the variations of the dc index with grating orders are similarly reported in [10]. On a similar note, the polarization characteristics of a uniform FBG depend on the refractive index profile along orthogonal polarization states over its grating period. With asymmetric (with respect to the cross-sectional area of the core) laser-induced grating pitches, the polarization characteristics are hence highly distinct. On the other hand, the wide pitch-to-pitch separation in the 2nd order grating structure helps to reduce the difference in the average index profile along orthogonal polarization states over a grating period. Consequently, the polarization-dependent spectral

#89342 - $15.00 USD Received 2 Nov 2007; revised 14 Dec 2007; accepted 15 Dec 2007; published 20 Dec 2007

responses from the 2nd order grating are less pronounced than that from the 1st order grating structure.

3. Application

In many fiber grating device applications, the effective manipulation of the polarization properties are often important practical factors for considerations. In particular for active grating resonators where spectral and polarization purity are of key concern, the presence of dual polarization longitudinal modes can generate undesired polarization mode beating signals and power instability due to polarization mode competition. Consequently, birefringent fibers and additional polarization-selective intra-cavity elements have been utilized to alleviate the issue. On the other hand, the spectral properties of the first-order C-band FBGs presented here can potentially offer a simple alternative to incorporate polarization-selectivity into grating resonators without adopting special fibers. For illustration, a Fabry-Perot (FP) FBG cavity was fabricated in a single-mode fiber (Corning SMF-28) by inscribing two 2.5mm-long uniform FBGs spaced 10mm apart. The one-step inscription process, synchronized to a shutter control, was carried out using a fixed fiber translation speed of 0.539mm/sec with measured inscription energy of 75nJ. The measured and simulated spectral profiles of the resultant FP cavity are as shown in Fig. 6.

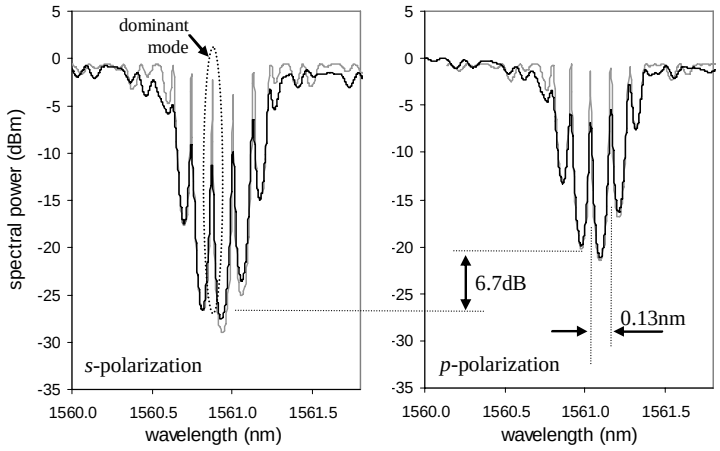

Fig. 6. Superimposed measured and simulated (grey) spectral transmission profiles of the Fabry-Perot first-order FBG cavity along orthogonal *s*- and *p*- polarization states.

Each resonance peak within the stopband width of the resonator cavity corresponds to a longitudinal mode with free spectral range measured 0.13nm. Likewise, the device response exhibits significant birefringence and polarization-dependent grating strength, determined by the grating reflectors. For each resonance mode, its constituent orthogonal polarization modes experience different reflectivity, hence amount of cavity feedback. As shown in Fig. 6, the dominant longitudinal mode (being closest to Bragg centre) exhibits differential transmission dip of ~6.7dB between orthogonal polarizations, denoted as *s*- and *p*-polarization. Resonance modes along the *s*-polarization hence experience stronger cavity feedback, therefore smaller cavity output coupling loss, than those along *p*-polarization. Given this loss being the key mode discrimination mechanism in active resonators, the differential cavity loss can hence lead to a dominant *s*-polarization mode operation. Furthermore, in line with previous studies [11], the grating coupling coefficients along orthogonal polarization states, denoted as κL_s and κL_p, satisfy the condition of $2\Delta\kappa L / (\kappa L_s + \kappa L_p) > 0.012$ (where $\Delta\kappa L = \kappa L_s - \kappa L_p$ and $\kappa L_p = 3.11$; $\kappa L_s = 3.95$). It can hence be deduced that such a fiber grating resonator is able to enforce

#89342 - $15.00 USD Received 2 Nov 2007; revised 14 Dec 2007; accepted 15 Dec 2007; published 20 Dec 2007

strong polarization-selectivity during operation. Further experimental verification of such active Fabry-Perot FBG devices will be carried out in gain fibers in near future.

4. Conclusion

In conclusion, high spectral quality FBGs with first-order Bragg resonances within the C-band are realized using point-by-point inscription technique with an IR femtosecond laser. The fabrication limitations imposed by the intrinsic fiber curvature are highlighted and resolved to realize closely-spaced grating periods (sub-μm) for FBG operating in the C-band. High degrees of polarization-dependency in the spectral responses are observed, which are potentially useful for short-length polarization-selective grating resonators. Further detail analysis of the grating polarization characteristics with different grating order and focusing conditions are to be carried out in near future.

#89342 - $15.00 USD Received 2 Nov 2007; revised 14 Dec 2007; accepted 15 Dec 2007; published 20 Dec 2007